Available Online at http://www.recentscientific.com

ISSN: 0976-3031

International Journal of Recent Scientific Research
Vol. 6, Issue, 7, pp.4956-4959, July, 2015

International Journal of Recent Scientific Research

RESEARCH ARTICLE

CHEMICALLY TREATED FERRIC NITRATE REINFORCED WITH SISAL FIBER: ITS STRUCTURE AND MORPHOLOGY

Asif jehan[1]*, Shirish joshi[2] and M.N. Bapat[3]

[1,3]Motilal Vigyan Mahavidhalya Bhopal (M.P.) India
[3]Regional Institute of Education Bhopal (M.P.) India

ARTICLE INFO

Article History:

Received 14th, June, 2015
Received in revised form 23th, June, 2015
Accepted 13th, July, 2015
Published online 28th, July, 2015

Key words:

Fe_2O_3, sintering method, XRD, SEM

ABSTRACT

Aluminum oxide synthesized through annealing route. The present research work deals with ferrite composite prepared using chemical reactions. Aluminum nitrates and ammonium chloride doped with sisal fiber has been prepared. The structural behavior of aluminum oxide was studied in XRD, and SEM. This behavior showed ferrite nature of the sample.

INTRODUCTION

The present contemporaries of Physicists and Engineers are focusing to reduce the operation of traditional fillers and increase the utilization of bio waste natural fiber material [1]. The syntheses of polymer based on composite materials have opened new traditions for the polymer fabrication and have allowed the manufacture of new products with optimal properties and its special applications [2]

$LiFeO_2$ has various crystalline structures such as α- $LiFeO_2$, β-$LiFeO_2$, γ-$LiFeO_2$, Layered $LiFeO_2$, Corrugated $LiFeO_2$, Goethite type $LiFeO_2$ etc. The crystalline structure of $LiFeO_2$ depends mainly on the preparation methods. Many researches prepared $LiFeO_2$ with different structures. V.R. Galakhov *et al.* prepared α-$LiFeO_2$ with Fm-3m space group by using solid state reaction and M. Tabuchi *et al*. prepared α-$LiFeO_2$ with Fm3m space group by hydrothermal synthesis [3-5]. Similarly, β-$LiFeO_2$, γ- $LiFeO_2$ and layered $LiFeO_2$ are prepared by hydrothermal synthesis and other methods. Corrugated $LiFeO_2$ and Goethite type $LiFeO_2$ are prepared by ion exchange method. In comparison with the conventional solid phase synthesis methods, hydrothermal method is one of the simplest and best methods to prepare lithium based cathode materials [6-9].In case of the electrical properties of the oxides, grain boundaries play an important role. The measurement of conductivity and permittivity shows dispersion behavior which offers an opportunity to gain some information of ionic migration process. Considering the significance, the electrical conductivity studies on various lithium-based oxides such as $LiCoO_2$, $LiCeO_2$, $LiSmO_2$, $Li2SnO_3$, $Li2MnO_3$, $LiMn_2O_4$, and $Li2V_2O_5$, and others have been reported in the literature [10-13]. However, to the best of our knowledge, there are meager reports on electrical and dielectric properties of $LiFeO_2$. A detailed study on the temperature and frequency depended electrical properties is necessary to understand the conduction mechanism in $LiFeO_2$ for effective utilization as cathode material in the fabrication of lithium ion batteries.

In the oxides of iron a-Fe_20_3 is the most stable compound. For the non-existence of Fe++ ions a-Fe_20_3 has higher electrical resistivity than other oxides of iron such as Fe_30_4, FeO, and ferrites. It has been reported, however, that at the temperature above 1200°C there is the possibility of the appearance of Fe++ ions in a-Fe_20_3. When the oxides contain ferrous ions, the hopping of electrons between ferrous and ferric ions gives rise to higher conductivity. Thus for samples possessing both the conductive and less-conductive phases the Maxwell-Wagner interfacial polarizations are observed. With the surface modified by the use of mild reducing condition of sintering Hirbon reported the interfacial polarization in the sintered compacts of a-Fe_20_3. On the other hand, in a-Fe203 containing other ions of different valences such as Ti" ions polarizations

*Corresponding author: **Asif jehan**
Motilal Vigyan Mahavidhalya Bhopal (M.P.) India

due to permanent dipoles of Fe++_Fe+++ induced by Ti+4 ions were observed at very low temperature [14-18]

In this paper a modest attempt has been made to unearth the abrasive wear behavior chemically treated sisal fibre composites by annealing treatment method. The sisal fibre is treated with inorganic nitrate salts. The treated surface of sisal fibre sample was characterized with the help of Scanning Electron Microscopy (SEM) technique and also by using the XRD analysis.

MATERIAL AND METHOD

Chemical treatment of fiber

Ferric Nitrate (Fe $(NO_3)_3.9H_2O$) and ammonium chloride (NH_4Cl) was taken in the ratio 10:4 in 500 *ml* of distilled water. The mixture was stirred till a homogenous solution was obtained. In this mixture 10g of sisal fiber was added and then 1:1 solution of NH_4OH (liquid ammonia) was added to it then left the solution for one hour. Again the mixture thus obtained was dried and then annealed in muffle furnace at 1000^oC and kept it at different time duration sample 1 (SP1) for 15 min, sample 2 (SP2) for 30 min and sample 3 (SP3) for 45 min.

The reaction may take place in this way
$2Fe(NO_3)_3.9H_2O+3NH_4Cl+3NH_4OH+Fiber \rightarrow Fe_2O_3$: $fiber+6NH_4NO_3 +3HOCl + 18H_2O$

When ferric nitrate reacts with ammonium chloride and ammonium hydroxide along with sisal fiber at 1000^{o}Cwith ammonium nitrate and HO-Cl (hypoclorous acid) decomposed at such high temperature and only ferric oxide is left.

Nature and structure of sample after firing

The material formed was found to in solid crystals in physical appearance. The sample appeared in powder form and it is like Cole in color.

RESULT AND DISCUSSION

XRD

The amorphous state of the sisal fiber composite was verified by XRD. The x-ray diffraction patterns of Fe_2O_3 doped with sisal fiber shown in fig 1, 2 & 3. The peaks for Fe_2O_3SP1 in fig 1 are observed at 2θ=10.744 (d=8.22775 Å), 2θ=24.164 (d=3.68020 Å), 2θ=33.190 (d=2.69705 Å), 2θ=35.663 (d=2.51552 Å), 2θ=40.913 (d=2.20401 Å), 2θ=49.508 (d=1.83965 Å), 2θ=54.127 (d=1.69305 Å), 2θ=57.717 (d=1.59599 Å), 2θ=62.497 (d=1.48491 Å), 2θ=64.067 (d=1.45226 Å) corresponding to (555), (562), (1032), (917), (611), (732), (713), (548), (649) and (648) reflections. The peaks present in Fe_2O_3 were also observed in the composition of sisal fiber with Fe_2O_3 which indicates the presence of ferrite particle. The entire pattern indicates about the small dimensions of the iron oxide particles. The changes in peaks occur due to the presence of composition of sisal fiber [18]. These radical cations through the coupling reaction lead to the ion of stable electrically conducting natural fiber. Reaction with the natural fiber generated by an internal redox reaction, which casus the reorganization of electronic structure to give the +ve and –ve nature of a radical is linked to its difference in reactivity towardslignin and cellulose/hemicelluloses [19].

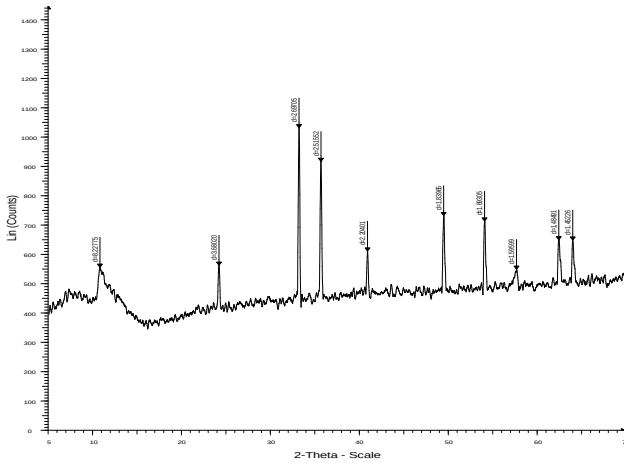

Fig 1

The peaks for Fe_2O_3SP2 in fig 2 are observed at 2θ=25.285 (d=3.5194 Å), 2θ=29.540 (d=3.0214 Å), 2θ=34.845 (d=2.5726 Å), 2θ=37.460 (d=2.3988 Å), 2θ=43.025 (d=2.1006 Å), 2θ=52.2008 (d=1.7509 Å), 2θ=57.180 (d=1.6097 Å), 2θ=66.170 (d=14111 Å), 2θ=67.845 (d=1.3803 Å), 2θ=76.520 (d=1.2439 Å) corresponding to (914), (269), (1629), (930), (1980), (888), (1725), (936), (1161) and (289) reflections. The peaks present in Fe_2O_3 were also observed in the composition of sisal fiber with Fe_2O_3 which indicates the presence of ferrite particle and the peaks for Fe_2O_3SP3 in fig 3 are observed at 2θ=25.330 (d=3.5133 Å), 2θ=34.890 (d=2.5694 Å), 2θ=37.505 (d=2.3960 Å), 2θ=43.075 (d=2.0982 Å), 2θ=52.225 (d=1.7489 Å), 2θ=57.225 (d=1.6085 Å), 2θ=61.000 (d=1.5177 Å), 2θ=66.220 (d=1.4101 Å), 2θ=67.220 (d=1.3794 Å), 2θ=76.585 (d=1.2430 Å) corresponding to (2296), (3887), (1915), (4481), (2112), (4019), (333), (1707), (2564) and (664) reflections. The peaks present in Fe_2O_3 were also observed in the composition of sisal fiber with Fe_2O_3 which indicates the presence of ferrite particle.

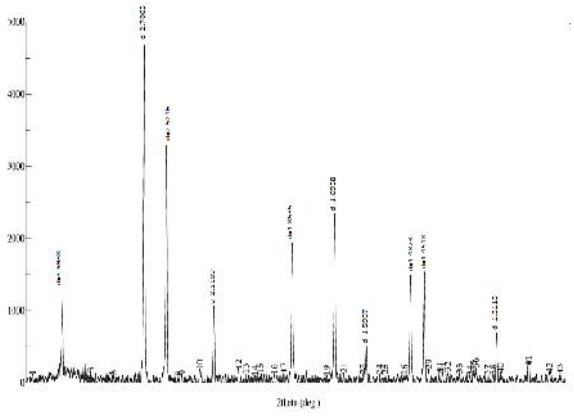

Fig 2

Natural sisal fiber consists of proton H+ molecule in its composition and deprotonation process is also occurred in natural fiber. Deprotonation is the removal of a proton (H+)

from a molecule. Deprotonation of the radical cation is a major pathway and the proton removal decreases positive charge in the molecule and an increases negative charge. Deprotonation usually occurs from the donation of electrons or acceptance of the proton using a base, which forms its conjugate acid [20].

Name	Symbol	Classification	A	B
Cellulose	$C_6H_{10}O_5$	C-H Deprotonation	C	H
Hemi-celluloses	$C_5H_{10}O_5$	C-H Deprotonation	C	H
Lignin	$C_{13}H_{34}O_{11}$	C-H Deprotonation	C	H

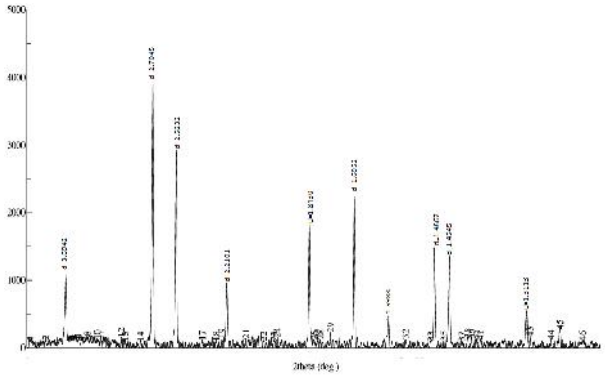

Fig 3

Some unknown peaks are present is the XRD graphs. Hence other crystalline phases such as various types of hydrated aluminum nitrate, ammonium chloride, sisal fiber or other impurities; might have been present in sample. Iron oxide cannot be produced at relatively very low temperature; therefore, it is not possible for nitrate ions to decompose. So that it's calcinated on high temperature at 1000^{o}C the 2θ peaks (or miller indices) which indicates that Al_2O_3 was present. As the time increased from 15 min (SP1), 30 min (SP2) and 45 min (SP3), the intensity of Al_2O_3 phase peaks of SP2 increased as compare to SP1 and peaks of SP3 decreased as compare to SP2. The XRD results do not show that the sample was hydrating salt with other impurities. Therefore water molecules and impurities already removed at this temperature. After being calcinated at 1000^{o}C the sample lost its crystalline structure and small amorphous humps appeared at 2θ= 8-12^o, 33-38^o and 53-64^{o}for SP1; 2θ= 11-13^o, 35-40^o and 56-61^o for SP2; 2θ= 11-12^o, 36-45^o and 55-60^{o}for SP3. These humps are due to the interference of XRD signals of iron oxide. At this temperature Al2o3 phases lose their bonding and appear highly amorphous in nature its intensity of humps increased. These results indicate that at this temperature the iron oxide particles in several crystallize iron oxide. These finding was confirmed by referring to the XRD data base reference data base (KSD collection code 025778). The crystal system of the structure was rhombohedral and had a density of 4.02cm^{-3}. The XRD peaks of SP2 and SP3 indicated the presence of α-iron oxide were at 2θ (miller indices) for SP2= 25.285, 29.540, 34.845, 43.025, 52.200, 57.180, 66.170, 67845, 76.520 and for SP3= 25.330, 34.890, 37.505, 43.075, 52.265, 57.225, 61.000, 66.220, 67.895, 76.585. Some of the reading has been verified due to impurities. The intensity of XRD peaks increased, indicating that more α-iron oxide crystals.

SEM

Figure 3 (a) and (b)shows the morphology ofFe_2O_3. The micrograph depicts the crystalline nature.The variation in specular optical transmittance against wavelengthfor pure and doped iron oxide. This shows the typical micrograph of the clustering of well-established randomly oriented nano rods which has compact, homogenous and well adherent growth onto the substrate. Fig (a) and (b) shows the morphology of material and fiber respectively. Fig 3(a) has porosity, non-uniform and inside hollow texture. Its upper surface is in crystalline, nonlinear, soft and spongy form. In fig 3(b) fiber shows a crystalline, linear and smoky effect.

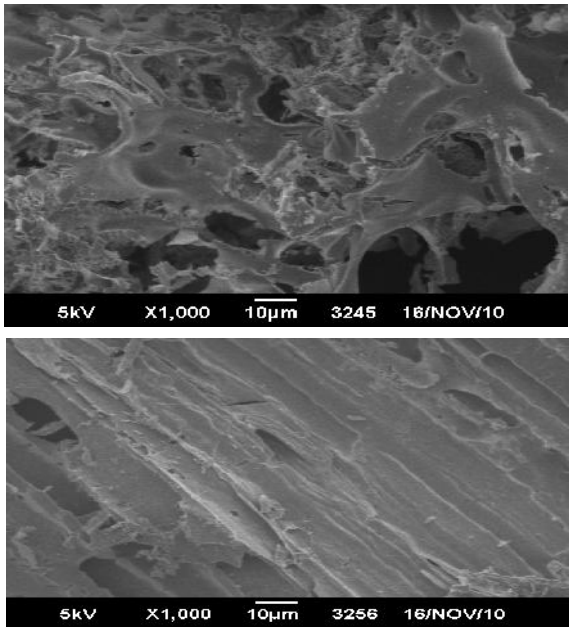

Fig 4

A change in the morphology and structure has been found after the treatment of sisal fibre which is confirmed by SEM technique. Figure 4, 5 & 6 shows the morphology ofFe_2O_3. The variations in specular optical transmittance against wavelength for pure and doped Aluminum oxide.

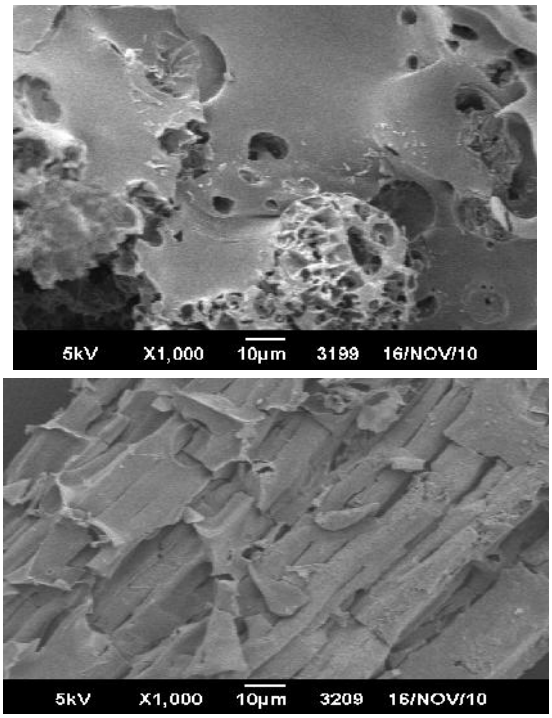

Fig 5

Uneven and cracked surface can be seen in the untreated samples which may be due to the presence of impurities in the fiber. The micrograph depicts the crystalline nature.This shows the typical micrograph of the clustering of well-established randomly oriented nano rods which has compact, homogenous and well adherent growth onto the substrate.

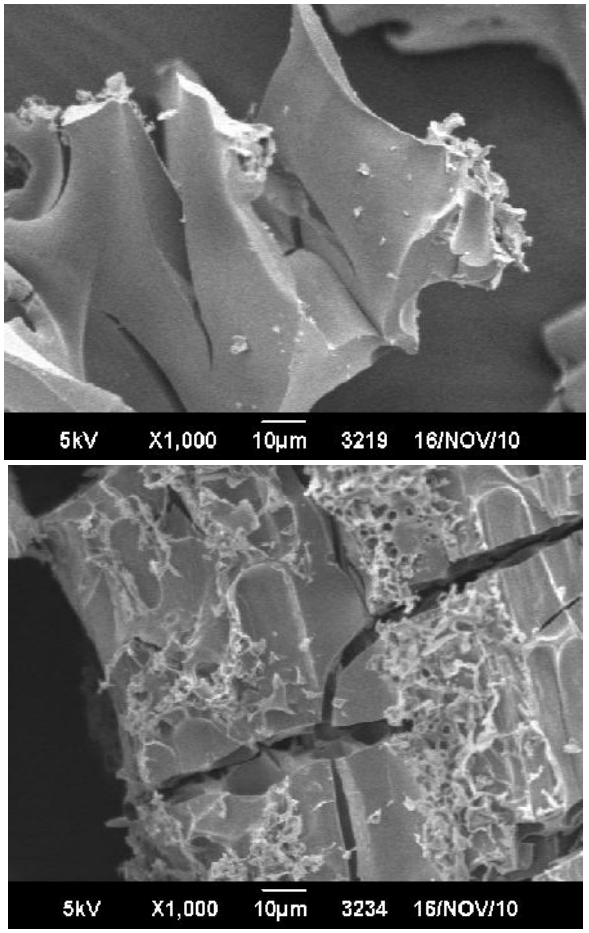

Fig 6

There was change in the unevenness of the surface in contrast of treated fiber it may be due to the chemical treatment done on the fiber. All images show the morphology of material and fiber respectively. Figures have porosity, non-uniform and inside hollow texture.

CONCLUSION

Calcinations of hydrated aluminum nitrate at high temperature eliminate steam, ammonium nitrate and dehydrate the aluminum nitrate and hypoclorous acid (volatile impurities). Calcinations dehydrate the aluminum nitrate salt and breakdown the nitrate ions at high temperature to produce α-iron oxide. Water molecules are released from the salt initially. Whereas other impurities released from salt at ~=1000^{o}C. The iron oxide is transformed to α-iron oxide after calcinations at temperature 1200^{o}C but because of sisal fiber and its impurities it converted in to α-iron oxide at temperature 1000^{o}C.

References

1. Ashutosh Tiwar.; Ajay Mishra, K.; Hisatoshi Kobayashi.; Anthony Turner, P.F. Wiley, USA, ISBN 978-04-709387-99, 2012.
ek *et al*. 1989
2. Galakhov, V.R.; Kurmaev, E.Z.; Uhlenbrock, S. Solid StateCommun. 1995, 95, 347.DOI: 10.1016/0038-1098(95)00279-0
3. George J., Sreekala, M. S., Thomas S.," A Review on Interface Modification and Characterization of Natural Fiber Reinforced Plastic Composites", Polymer Engg. and Sci., Vol. 41, pp. 1471-1485, (2001).
4. J. C. Maxwell, Electricity and Magnetism, Oxford University Press, London (1873), vol. 1, Sec. 328.
5. K. W. Wagner, Ann. Physik, 40, 817 (1913); Arch Electroch. 2, 371 (1914).
6. Lee, Y.S.; Sato, S.; Tabuchi, M. Electrochem. Commun. 2003, 5,549.DOI: 10.1016/S1388-2481(03)00118-8
7. Lee, Y.S.; Sato, S.; Tabuchi, M.; Yoon, C.S.; Sun, Y.K.;Kobayakawa, K.; Sato, Y. lectrochem. Commun. 2003, 5, 549.DOI: 10.1016/S1388-2481(03)00118-8
8. Masaaki Hirayama.; Hiroki Tomita.; Kei Kubota.; Ryoji Kanno.; J.Power Sources 2011, 196, 809.DOI: 10.1016/j.jpowsour.2010.10.009
9. Michele Catti.; Merced Montero-Campillo.; J. Power Sources 2011,196, 3955. DOI: 10.1016/j.jpowsour.2010.11.062
10. P. M. Hansen, Constitution of Binary Alloys, McGraw Hill Book Company New York, (1958) 688.
11. Prabu, M.; Selvasekarapandian, S.; Kulkarni, A. R; Hirankumar, G.; Sakunthala. A. Solid State Ionics 2010, 16, 317. DOI : 10.1007/s11581-010-0420-7
12. Prabu, M.; Selvasekarapandian, S.; Kulkarni, A.R.; Hirankumar , G.; Sanjeeviraja, C. J. Rare Earths 2010, 28, 435. DOI: 10.1016/S1002- 721(09)60128-9
13. R. B. Hirborn, J. App. Phys. 36, 1553 (1965).
14. s.k. dhawan kuldeep singh, anil, a.k. bakhshi polymeric & soft materials section. National physical laboratory. New delhi-110021. India
15. Santos-Pena, J.; Crosinier, O.; Brousse, T. Electrochimica Acta2010, 55, 7511.DOI: 10.1016/j.electacta.2009.12.069
16. Schmittle, M.; Burghart, A. Angew. Chem. int. Ed. EEngl.1997,36,2550.
17. Son J. I., Kim H.J., Lee P. W., Role of Paper Sludge Particle Size and Extrusion; "Temperature on Performance of Paper Sludge Thermoplastic Polymer Composites" Journal of Appl. Polymer Sci., Vol. 82 (11), pp. 2709-2718, (2001).
18. Sung-Woo Kim,.; Su-Il Pyun. J. Electroanalytical. Chem. 2002, 528, 114.DOI: S0022-0728(02)00900
19. Vijayakumar, M.; Selvasekarapandian, S.; Kesavamoorthy, R.; Koichi Nakamura.; Tatsuo Kanashiro. Mater. Lett. 2003, 57, 3618. DOI: 10.1016/S0167-577X(03)00137-X

How to cite this article:
Asif jehan *et al*., Chemically Treated Ferric Nitrate Reinforced With Sisal Fiber: Its Structure And Morphology. *International Journal of Recent Scientific Research Vol. 6, Issue, 7, pp.4956-4959, July, 2015*